

Effect of 90° Domain Walls on the Low-Field Permittivity of $\text{PbZr}_{0.2}\text{Ti}_{0.8}\text{O}_3$ Thin Films

J. Karthik, A. R. Damodaran, and L. W. Martin*

Department of Materials Science and Engineering and Materials Research Laboratory, University of Illinois, Urbana-Champaign, Urbana, Illinois 61801, USA

(Received 26 October 2011; revised manuscript received 19 January 2012; published 16 April 2012)

We report on the contribution of 90° ferroelastic domain walls in strain-engineered $\text{PbZr}_{0.2}\text{Ti}_{0.8}\text{O}_3$ thin films to the room-temperature permittivity. Using a combination of phenomenological Ginzburg-Landau-Devonshire polydomain thin-film models and epitaxial thin-film growth and characterization, the extrinsic or domain wall contribution to the low-field, reversible dielectric response is evaluated as a function of increasing domain wall density. Using epitaxial thin-film strain we have engineered a set of samples that possess a known quantity of 90° domain walls that act as a model system with which to probe the contribution from these ferroelastic domain walls. We observe a strong enhancement of the permittivity with increasing domain wall density that matches the predictions of the phenomenological models. Additionally, we report experimentally measured bounds to domain wall stiffness in such $\text{PbZr}_{0.2}\text{Ti}_{0.8}\text{O}_3$ thin films as a function of domain wall density and frequency.

DOI: [10.1103/PhysRevLett.108.167601](https://doi.org/10.1103/PhysRevLett.108.167601)

PACS numbers: 77.22.Ch, 77.55.fg, 77.80.Dj, 81.15.Fg

Domains and domain walls are known to dramatically impact the properties of ferroic materials. In ferroelectrics, for instance, the morphology of the domains generally results in a configuration that minimizes the sum of elastic and electrostatic energies, but is known to depend on the material structure, the presence of surfaces and interfaces, the elastic and thermal history, electrical boundary conditions, and more [1]. Such domain structures can have a profound effect on the dielectric [2–4], piezoelectric [3,4], and pyroelectric [5] susceptibilities of ferroelectrics. This is due to the displacement of domain walls under external stimuli (e.g., electric field, stress, and temperature) that gives rise to a so-called extrinsic contribution to the susceptibilities in addition to the intrinsic response of the polarization. For small excitation amplitudes, the extrinsic contribution is reversible and independent of the excitation amplitude; however, for larger excitations irreversible motion of domain walls gives rise to an amplitude dependent contribution [6,7]. Even in the reversible regime, these extrinsic contributions have been predicted to give rise to large room-temperature susceptibilities near strain- and thickness-induced transformations in polydomain structures [4,8,9].

Researchers have long recognized the important role of domain walls in determining the permittivity of polydomain ferroelectrics [10–12]. A number of experimental studies (focused on bulk ceramics and polycrystalline films) have examined domain wall contributions to permittivity [3,4,9,13]. Using low-temperature measurements, for instance, researchers “froze-out” the domain wall contribution and found 25%–50% of the room-temperature response arising from extrinsic effects [3]. Studies of textured, polycrystalline films suggested that the extrinsic contribution to the room-temperature permittivity was dominated by 180° domain wall motion and that 90°

domain walls were important only in large grained films [4]. Furthermore, it has been observed that 90° domain wall motion is substantially smaller in $\text{PbZr}_{1-x}\text{Ti}_x\text{O}_3$ (and other perovskite) thin films than in bulk ceramics of the same composition [4,13–15]. Recent work on polycrystalline $\text{PbZr}_{1-x}\text{Ti}_x\text{O}_3$ thin films has, however, suggested that stress-driven motion of 90° domain walls can occur and gives rise to strong direct piezoelectric response [16,17].

Models [8,18–20] have also predicted enhancement of the room-temperature permittivity in ferroelectric thin films possessing 90° domain walls. First-principles calculations [21] have shown that 90° domain walls should have a lower lattice barrier for their translational motion due to their larger width and should contribute significantly to dielectric properties near room temperature. The importance of these 90° domain walls is further enhanced since they are very common in ferroelectric capacitor structures that are commonly used in practical applications [20,22]. Quantitative investigation of the effect of 90° domain walls on the permittivity, however, has proved difficult to obtain due to the presence of grain boundaries and a mixture of domain wall types in many ferroelectric samples.

In this Letter, we use a combination of theoretical and experimental approaches to directly probe the effect of 90° domain walls on the room-temperature permittivity of $\text{PbZr}_{0.2}\text{Ti}_{0.8}\text{O}_3$ thin films and unequivocally demonstrate how the reversible motion of these domain walls can dramatically enhance dielectric permittivity. Using epitaxial thin-film strain, we have tuned the domain structure and the resulting permittivity of the films. Comparisons to polydomain models reveal strong similarities and in-depth experimental analysis enables us to extract the domain wall contribution to the permittivity, relate the measured effects to the microscopic details of the domain wall response under applied electric fields, and experimentally measure

domain wall stiffness. This highlights the importance of domain walls to the room-temperature permittivity and provides a realistic comparison between models and experiment.

Domain formation has long been recognized as a ubiquitous mechanism for strain relief during the epitaxial growth of ferroelectric films [23–25]. The epitaxial strain due to the substrate is relieved by the formation of a twinned structure with domains oriented with their tetragonal axis essentially parallel (c domains) and perpendicular (a domains) to the (001) substrate normal [26,27]. The relative abundance of domains of each type depends on the misfit strain, film thickness, and the temperature. In general, increasing tensile strain increases the fraction of the a domains and the most common of such domain structures consists of an alternating array of c and a domains separated by 90° domain walls that are oriented at $\sim 45^\circ$ to the substrate normal (referred to here as $c/a/c/a$).

In order to understand the effect of these domain walls on the physical properties, we consider a tetragonal ferroelectric film of $\text{PbZr}_{0.2}\text{Ti}_{0.8}\text{O}_3$ grown epitaxially on a (001)-oriented cubic substrate. The equilibrium domain structure of the film at a given misfit strain can be predicted using polydomain Ginzburg-Landau-Devonshire (GLD) models for dense domain structures [5,20,22]. Assuming homogeneous strain fields inside the domains and neglecting the domain wall self-energies and interdomain electrostatic interactions, we can write a free energy for the system in terms of the polarization and domain fractions while taking into account the coupling between strain and polarization. By minimizing the free energy with the in-plane strain imposed by the substrate and by applying short-circuit electrical boundary conditions we can calculate the equilibrium polarizations (P_1, P_2, P_3) and domain fractions as a function of the misfit strain.

From such a calculation at 300 K, we see that at large compressive strains the film is monodomain with the c axis along the substrate normal [left, Fig. 1]. On reducing the compressive strain it undergoes an elastically driven relaxation to the $c/a/c/a$ domain structure with an increasing fraction of a domains with increasing tensile strain [center, Fig. 1]. At a critical tensile strain, the c domains vanish and the film adopts the $a_1/a_2/a_1/a_2$ domain structure. This transformation from $c \rightarrow c/a/c/a \rightarrow a_1/a_2/a_1/a_2$ is accompanied by a corresponding change in the out-of-plane permittivity (ϵ_{33}) which can be evaluated as

$$\epsilon_{33} = \frac{d\langle P_3 \rangle}{dE} = \phi_c \frac{dP_3}{dE} + P_3 \frac{d\phi_c}{dE}, \quad (1)$$

where P_3 , ϕ_c , and E represent the out-of-plane polarization, the fraction of the c domains, and the electric field along the substrate normal, respectively. The first term represents the intrinsic permittivity of the polydomain state and the second term is the extrinsic contribution to the

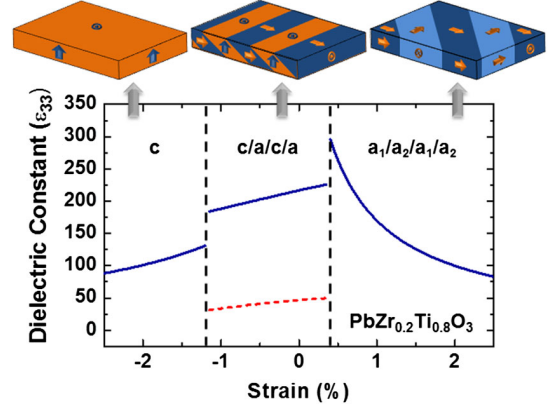


FIG. 1 (color online). Schematic illustration of predicted ferroelectric domain structure in various strain regimes for $\text{PbZr}_{0.2}\text{Ti}_{0.8}\text{O}_3$ thin films and corresponding strain-dependent evolution of room-temperature permittivity. Solid line shows intrinsic plus extrinsic contributions and dashed line shows the intrinsic contribution alone.

permittivity arising from the reversible displacement of the domain walls that changes the domain fractions. In the linear approximation (valid at low electric fields), neglecting the effect of small domain wall displacement on the polarization within the domains, we can calculate the extrinsic contribution to the permittivity analytically as [20]

$$\epsilon_x = \frac{(s_{11}^2 - s_{12}^2)}{s_{11}(Q_{11} - Q_{12})^2 P_s^2}, \quad (2)$$

where s_{ij} are the elastic compliances, Q_{ij} are the electrostrictive coefficients, and P_s is the spontaneous polarization within each domain such that the average polarization along the substrate normal $\langle P_3 \rangle = \phi_c P_s$. We find that the intrinsic permittivity [dashed line, Fig. 1] of the polydomain $c/a/c/a$ state is < 100 and that the total permittivity [solid line, Fig. 1] (intrinsic plus extrinsic contributions) is expected to be enhanced. Furthermore, the extrinsic contribution increases with increasing fraction of the a domains (and tensile strain) until the film transforms to the completely in-plane polarized $a_1/a_2/a_1/a_2$ state.

In order to investigate the effect of 90° domain walls on the permittivity, we have grown 150 nm $\text{PbZr}_{0.2}\text{Ti}_{0.8}\text{O}_3/20$ nm SrRuO_3 heterostructures on $\text{SrTiO}_3(001)$, $\text{DyScO}_3(110)$, $\text{TbScO}_3(110)$, and $\text{GdScO}_3(110)$ using pulsed-laser deposition [28]. In order to measure the dielectric and ferroelectric properties of the thin-film heterostructures, capacitor structures were fabricated with 80 nm thick epitaxial SrRuO_3 top electrodes (circular capacitors, diameter 50–100 μm) [29]. Capacitance-voltage and polarization-electric field hysteresis loops were measured at 1–100 kHz to characterize the dielectric and ferroelectric response. In order to measure the dielectric constant in the reversible regime a small AC excitation of 0.1 V was used.

The chosen substrates provide lattice mismatches with the $\text{PbZr}_{0.2}\text{Ti}_{0.8}\text{O}_3$ of -0.8% , 0.2% , 0.6% , and 0.9% for

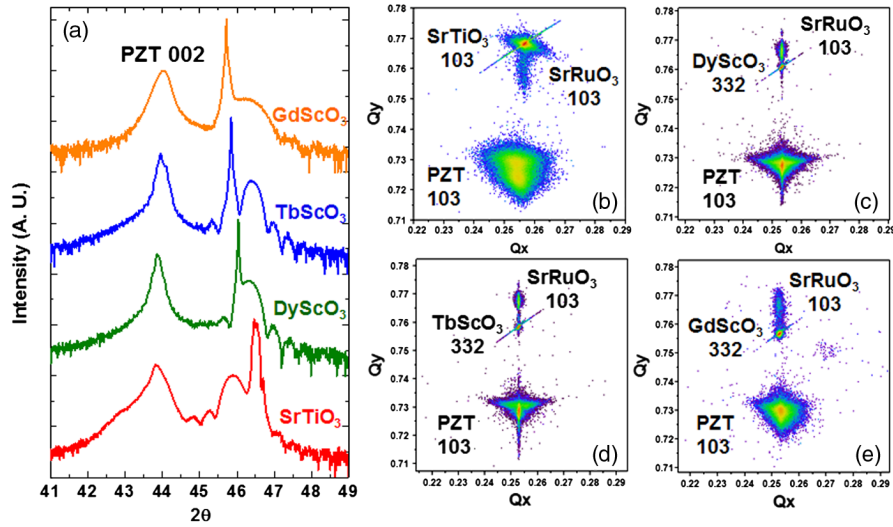


FIG. 2 (color online). (a) θ - 2θ x-ray diffraction patterns about the 002-diffraction peaks for various thin-film heterostructures reveal single-phase, epitaxial films. Reciprocal space maps about the pseudocubic 103-diffraction conditions for heterostructures grown on (b) SrTiO₃ (001), (c) DyScO₃ (110), (d) TbScO₃ (110), and (e) GdScO₃ (110).

SrTiO₃, DyScO₃, TbScO₃, and GdScO₃, respectively. Atomic force microscopy (AFM) of as-grown films revealed smooth surfaces (Suppl. Fig. S1 [30]). Detailed x-ray diffraction (XRD) studies reveal single-phase, fully epitaxial thin films [Fig. 2(a)]. Off-axis reciprocal space maps (RSMs) about the 103-pseudocubic diffraction condition revealed that the c -domain portion of the heterostructures are coherently strained to the underlying substrate in all cases [Figs. 2(b)–2(e)]. The GLD models predict that the fraction of a domains will increase with increasing tensile strain and this increase in the fraction of a domains was observed using a combination of XRD, AFM, and piezoresponse force microscopy (PFM). Rocking curve and RSM studies of the 200-diffraction peaks of all films reveal a strong increase in the intensity of these peaks with increasing tensile strain [Suppl. Fig. S2 [30]]. Using standard XRD rocking curve analysis [26] [Suppl. Fig. S2 [30]] and PFM studies [Suppl. Fig. S3 [30]] we have estimated the fraction of the a domains [Table I]. The PFM studies also allow us to directly measure the average domain periodicity [D , Table I]. We note that detailed PFM investigations reveal no 180° domain walls in these films consistent with prior studies of ferroelectric films with asymmetric electrical boundary conditions that stabilize a preferential direction for polarization [31,32]. These analyses reveal that films under strong compressive strain (e.g. on SrTiO₃) are essentially completely c -axis oriented ($\phi_a \sim 4\%$) while films under mild tensile strain (e.g., on GdScO₃) possess $\phi_a \sim 20\%$. Remnant polarization (P_r) was extracted from hysteresis loops and PUND measurements [Suppl. Fig. S4(a),(b) [30]] and are reported in Table I. Values of P_r are consistent with prior reports of high spontaneous polarization in high-quality PbZr_{0.2}Ti_{0.8}O₃ films [33].

We note that the ϕ_a observed experimentally deviates slightly from those predicted by the polydomain GLD model which predicts the onset of the $a_1/a_2/a_1/a_2$ domain structure for films grown on GdScO₃. This is likely due to the simplifying assumptions applied in the polydomain GLD model and to the finite thickness of our films. Phase-field models, which account for interdomain electrostatic interactions and make no *a priori* assumptions about the domain structure, predict a transition to the fully in-plane oriented $a_1/a_2/a_1/a_2$ state at larger tensile strains than the current models [22,34]. Further, the lack of complete local charge compensation at the domain walls could lead to an increased stability of the c domains [34]. Charge compensation mechanisms are dependent on the processing conditions thus it is unreasonable to expect theoretical models to exactly predict the experimentally observed strain dependence. Regardless, the values of permittivity (and other thermodynamic properties) predicted from these polydomain GLD models do show the correct trends. ϕ_a is also a function of the film thickness and it is expected to increase with increasing thickness, but we have focused here on 150 nm thick films in order to maintain coherently strained c domains in the films. Since we can directly

TABLE I. Fraction of a domains (ϕ_a), domain periodicity (D), remnant polarization (P_r), and domain wall stiffness (k) as measured for film grown on various substrates.

Substrate	ϕ_a %	D (μm)	P_r ($\mu\text{C}/\text{cm}^2$)	k (10^{15} N/m ³)	
				10^3 Hz	10^5 Hz
SrTiO ₃ (001)	4.2	2.72	90	0.58	0.75
DyScO ₃ (110)	9.3	2.72	78	0.45	0.56
TbScO ₃ (110)	11.2	1.80	73	0.63	0.78
GdScO ₃ (110)	20.2	0.59	61	1.59	1.76

measure ϕ_a and D we can relate the effect of domain structure to the physical properties without any *a priori* assumptions about the domain distributions.

Using the symmetric capacitor structures, we undertook extensive electrical characterization. Note that capacitors showing nearly symmetric current-voltage response, negligible imprint in the hysteresis loops, and low loss tangents were used for this study [Suppl. Fig. S4 [30]]. The relationship between the experimentally measured polarization and ϕ_a are also plotted as a function of epitaxial strain [Suppl. Fig. S5 [30]]. The permittivity is observed to increase with increasing ϕ_a [Fig. 3]. Again, studies were completed at small AC excitations to assure that the permittivity was measured in the reversible regime [Suppl. Fig. S6 [30]] and on all four substrate types the permittivity shows a significant frequency dispersion [Suppl. Fig. S7 [30]]. The frequency dependence of the dielectric constant is likely due to two important factors. First, although some reports suggest that the domain wall contribution should be frequency independent up to the domain wall resonance (1–10 GHz), in practice, the finite depinning time of the domain walls gives rise to a logarithmic frequency dependence in the low frequency regime [35–37]. Second, point defects, such as oxygen vacancies, are also known to contribute significantly to the low frequency (< 100 kHz) permittivity and their contribution decreases with increasing frequency [37–39]. Since these two effects are intimately connected and almost always present in any real material (be it films, bulk ceramics, or single crystals), it is very difficult to separate these two effects in any study of these materials. We note, however, that the trends in the measured permittivity agree well with the predictions of the GLD theory [solid line, Fig. 3].

To gain a deeper understanding into the observed dielectric behavior and of the domain wall motion, one can describe the field induced vibrations of the domain walls using standard equations of motion [2,8]. Generally for a

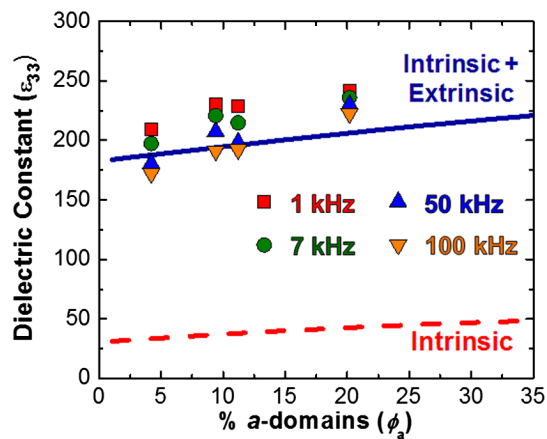


FIG. 3 (color online). Dielectric permittivity as a function of percentage a domains in polydomain $\text{PbZr}_{0.2}\text{Ti}_{0.8}\text{O}_3$ thin films measured at various frequencies.

90° domain wall at low frequencies, the mass of the domain wall is neglected and the restoring force (F_r) can be written in terms of a domain wall stiffness k defined as $F_r = -kl$ where l is the amplitude of the field induced domain wall oscillations. Thus, the domain wall contribution to the permittivity can be written as $\epsilon_x = \frac{2\sqrt{2}P_s^2}{\epsilon_0 k D}$ [8]. The concept of stiffness has been invoked for many years [2,8,18,40] to understand the behavior of domain walls, but it is usually treated as an adjustable parameter which is fitted to the experimental results. Additionally, there are conflicting reports as to the effect of domain size on k [18,41] and since domain wall pinning is typically neglected in theoretical approaches, this naturally lead to a frequency independent k . In real samples, however, k is frequency dependent even in the 1–100 kHz regime due to pinning and our measurements allow us to extract a lower bound to the domain wall stiffness at the two bounding frequencies [Table I]. To date, no experimental values for k have been reported in the literature and it is difficult to find values from theoretical treatments. Provided enough information, however, one can estimate values of k from parameters such as domain size, grain size, spontaneous polarization, permittivity, elastic stiffness, etc. From prior studies [18], we can estimate k values of 10^{14} N/m³. This is consistent with what we observe for samples with low densities of domain walls. We note, however, that k values increase with increasing density of domain walls and could be dramatically underestimated (by at least an order of magnitude) in samples possessing $\phi_a > 20\%$. This has considerable implications for estimates of thermodynamic quantities near the tensile-strain-induced phase boundary and for overall estimates of domain wall contributions to physical properties.

This work offers unique insight into the microscopic coupling between electric fields and domain walls in ferroelectrics. In tetragonal ferroelectrics that can have both 180° (ferroelectric) and 90° (ferroelastic) domain walls, it has been suggested that 180° domain wall motion will affect only the permittivity and 90° domain wall motion will affect both dielectric and piezoelectric properties. Although some work has been done concerning the effect of 90° domain walls on piezoelectric properties in films [16,17,42], prior studies of effects on permittivity were obscured by complex polycrystalline structures and the resulting complex interplay of domain walls and grain boundaries. We have generated a model set of epitaxial thin films that closely match polydomain GLD models and have observed the unambiguous contribution of 90° domain walls to dielectric response at room temperature and experimentally probed domain wall stiffness.

J. K. and L. W. M. acknowledge support from the Office of Naval Research under Grant Number N00014-10-10525. A. R. D. and L. W. M. acknowledge support from the Army Research Office under grant W911NF-10-1-0482. Experiments were carried out in part in the

Frederick Seitz Materials Research Laboratory Central Facilities, which are partially supported by the U.S. Department of Energy under grants DE-FG02-07ER46453 and DE-FG02-07ER46471.

*lw martin@illinois.edu

- [1] D. Li and D. A. Bonnelli, *Annu. Rev. Mater. Res.* **38**, 351 (2008).
- [2] N. A. Pertsev, G. Arlt, and A. G. Zembilgotov, *Microelectronics Engineering* **29**, 135 (1995).
- [3] Q. M. Zhang, H. Wang, N. Kim, and L. E. Cross, *J. Appl. Phys.* **75**, 454 (1994).
- [4] F. Xu, S. Trolier-McKinstry, W. Ren, B. Xu, Z.-L. Xie, and K. J. Hemker, *J. Appl. Phys.* **89**, 1336 (2001).
- [5] J. Karthik and L. W. Martin, *Phys. Rev. B* **84**, 024102 (2011).
- [6] O. Boser, *J. Appl. Phys.* **62**, 1344 (1987).
- [7] G. Bertotti and I. Mayergoyz, *The Science of Hysteresis* (Academic, New York, 2005), Vol. 3.
- [8] N. A. Pertsev, G. Arlt, and A. G. Zembilgotov, *Phys. Rev. Lett.* **76**, 1364 (1996).
- [9] D.-J. Kim, J. P. Maria, A. I. Kingon, and S. K. Streiffer, *J. Appl. Phys.* **93**, 5568 (2003).
- [10] K. W. Plessner, *Proc. Phys. Soc. London* **69**, 1261 (1956).
- [11] B. Lewis, *Proc. Phys. Soc. London* **73**, 17 (1959).
- [12] C. Kittel, *Phys. Rev.* **83**, 458 (1951).
- [13] N. Bassiri-Gharb, I. Fujii, E. Hong, S. Trolier-McKinstry, D. V. Taylor, and D. Damjanovic, *J. Electroceram.* **19**, 49 (2007).
- [14] B. A. Tuttle, T. J. Garino, J. A. Voight, T. J. Headley, D. Dimos, and M. O. Eatough, *Science and Technology of Electroceramic Thin Films*, edited by O. Auciello, R. Waser (Kluwer, The Netherlands, 1995), 117–132.
- [15] J. F. Shepard, Jr., F. Chu, B. Xu, and S. Trolier-McKinstry, *Mater. Res. Soc. Symp. Proc.* **493**, 81 (1997).
- [16] A. Pramanick, D. Damjanovic, J. E. Daniels, J. C. Nino, and J. L. Jones, *J. Am. Ceram. Soc.* **94**, 293 (2011).
- [17] R. J. Zednik, A. Varatharajan, M. Oliver, N. Valanoor, and P. C. McIntyre, *Adv. Funct. Mater.* **21**, 3104 (2011).
- [18] G. Arlt and N. A. Pertsev, *J. Appl. Phys.* **70**, 2283 (1991).
- [19] A. Erbil, Y. Kim, and R. A. Gerhardt, *Phys. Rev. Lett.* **77**, 1628 (1996).
- [20] V. G. Koukhar, N. A. Pertsev, and R. Waser, *Phys. Rev. B* **64**, 214103 (2001).
- [21] B. Meyer and D. Vanderbilt, *Phys. Rev. B* **65**, 104111 (2002).
- [22] V. G. Koukhar, N. A. Pertsev, H. Kohlstedt, and R. Waser, *Phys. Rev. B* **73**, 214103 (2006).
- [23] A. L. Roitburd, *Phys. Status Solidi A* **37**, 329 (1976).
- [24] B. S. Kwak, A. Erbil, B. J. Wilkens, J. D. Budai, M. F. Chrisholm, and L. A. Boatner, *Phys. Rev. Lett.* **68**, 3733 (1992).
- [25] C. M. Foster, W. Pompe, A. C. Daykin, and J. S. Speck, *J. Appl. Phys.* **79**, 1405 (1996).
- [26] V. Nagarajan, I. G. Jenkins, S. P. Alpay, H. Li, S. Aggarwal, L. Salamanca-Riba, A. L. Roytburd, and R. Ramesh, *J. Appl. Phys.* **86**, 595 (1999).
- [27] N. A. Pertsev and A. G. Zembilgotov, *J. Appl. Phys.* **80**, 6401 (1996).
- [28] The SrRuO₃ and PbZr_{0.2}Ti_{0.8}O₃ layers were fabricated by pulsed laser deposition employing a KrF excimer laser (wavelength $\lambda = 248$ nm) from ceramic SrRuO₃ and PbZr_{0.2}Ti_{0.8}O₃ targets (Praxair Specialty Ceramics). The SrRuO₃ layer (20 nm) was deposited at 630 °C in an oxygen pressure of 100 mTorr, with a laser fluence of 1.75 J/cm² at a laser repetition rate of 12 Hz. The subsequent PbZr_{0.2}Ti_{0.8}O₃ layer (150 nm) was grown at 630 °C in an oxygen pressure of 200 mTorr at a laser fluence of 2 J/cm² and a laser repetition rate of 3 Hz.
- [29] J. Karthik, A. R. Damodaran, and L. W. Martin, *Adv. Mater.* **24**, 1610 (2012).
- [30] See Supplemental Material at <http://link.aps.org/supplemental/10.1103/PhysRevLett.108.167601> for details.
- [31] C.-L. Jia, V. Nagarajan, J.-Q. He, L. Houben, T. Zhao, R. Ramesh, K. Urban, and R. Waser, *Nature Mater.* **6**, 64 (2007).
- [32] L. W. Martin, Y.-H. Chu, M. B. Holcomb, M. Huijben, P. Yu, S.-J. Han, D. Lee, S. X. Wan, and R. Ramesh, *Nano Lett.* **8**, 2050 (2008).
- [33] I. Vrejoiu, G. Le Rhun, L. Pintilie, D. Hesse, M. Alexe, and U. Gösele, *Adv. Mater.* **18**, 1657 (2006).
- [34] G. Sheng, J. X. Zhang, Y. L. Li, S. Choudhury, Q. X. Jia, Z. K. Liu, and L. Q. Chen, *J. Appl. Phys.* **104**, 054105 (2008).
- [35] D. Damjanovic, *Phys. Rev. B* **55**, R649 (1997).
- [36] N. Bassiri-Gharb and S. Trolier-McKinstry, *J. Appl. Phys.* **97**, 064106 (2005).
- [37] V. Porokhonskyy, L. Jin, and D. Damjanovic, *Appl. Phys. Lett.* **94**, 212906 (2009).
- [38] S.-J. Lee, K.-Y. Kang, and S.-K. Han, *Appl. Phys. Lett.* **75**, 1784 (1999).
- [39] I. W. Kim, C. W. Ahn, J. S. Kim, T. K. Song, J.-S. Bae, B. C. Choi, J.-H. Jeong, and J. S. Lee, *Appl. Phys. Lett.* **80**, 4006 (2002).
- [40] G. Arlt and H. Dederichs, *Ferroelectrics* **29**, 47 (1980).
- [41] G. Arlt, D. Hennings, and G. de With, *J. Appl. Phys.* **58**, 1619 (1985).
- [42] G. Le Rhun, I. Vrejoiu, and M. Alexe, *Appl. Phys. Lett.* **90**, 012908 (2007).